J. Fluid Mech. (1976), *vol.* 77, *part* 2, *pp.* 257–277
Printed in Great Britain

Spectral analogy between temperature and velocity fluctuations in a turbulent boundary layer

By L. FULACHIER AND R. DUMAS

Institut de Mécanique Statistique de la Turbulence,
Université d'Aix-Marseille, 12 Avenue Général Leclerc, 13003 Marseille, France

(Received 3 March 1975 and in revised form 9 February 1976)

Experiments were carried out in the turbulent boundary layer on a slightly heated plate in order to establish, mainly for the larger scales of motion, any analogy that may exist between the temperature and velocity fluctuations. With this goal in mind, the spectra and cospectra of the temperature and velocity fluctuations were measured. In particular, the cospectra were obtained by the 'fluctuation-diagram method'. It soon became evident that the temperature spectrum, except very close to the wall, differs strongly from the spectrum of the longitudinal velocity component. At least for the lower frequency spectral range, which includes about 80% of the total variance, the experimental results support an analogy between the temperature spectrum and a new type of spectrum consisting of the sum of the spectra of the three velocity components weighted by their relative energy. This analogy was established throughout most of the boundary layer.

1. Introduction

In turbulent flows, Reynolds (1874) has proposed that the mechanisms for turbulent transport of the momentum and heat are the same. This 'Reynolds analogy' has been used to compute the mean temperature distribution from the mean velocity distribution in the case of quasi-parallel flows (Ribaud & Brun 1942; Howarth 1953; Eckert & Drake 1959). Furthermore, if the boundary conditions for momentum and heat are also analogous, the mean velocity and temperature profiles must be similar (Kestin & Richardson 1963).

Now the question arises whether it is possible to establish an analogy between the temperature and velocity fluctuations. Here we are concerned only with slow subsonic flows that are heated slightly, so that both the Mach number and the Richardson number are very small and the buoyancy and compressibility effects, at least for the fluctuations, are essentially negligible. One may refer to Favre (1975) for a discussion of the thermal effects on the velocity field.

Prior to the present work the following facts were considered established.

(*a*) Under the above stated experimental conditions, heat is considered as a passive scalar contaminant.

(*b*) It has been shown that (Corrsin 1951; Batchelor 1952; Lumley & Panofsky 1964) the temperature fluctuation field does not propagate in the ordinary

sense but is transported by the total velocity, and the molecular diffusion smooths out only the small-scale turbulent temperature fluctuations.

(*c*) For the present case, an analogy cannot be obtained from the total enthalpy equation, namely from the adiabatic relation often used in steady compressible flows: $c_p\theta' + \bar{u}_1 u_1' = 0$, where θ' is the temperature fluctuation and u_1' the longitudinal velocity fluctuation. The main reason is that the variations in temperature are not due to those in the velocity but arise owing to the external heat flux. Here the temperature fluctuations correspond essentially to the entropy fluctuations (Favre, Dumas & Verollet 1968).

(*d*) In quasi-parallel turbulent shear flows such as a two-dimensional boundary layer, only one mean velocity component is important, the other two being negligible. Nevertheless such considerations do not apply to the velocity fluctuation field. Indeed, except very close to the wall, the intensities of the three components of the velocity are of the same order of magnitude.

There is ample experimental evidence that the temperature fluctuation is strongly correlated both with the streamwise velocity component u_1' and also with the normal velocity component u_2', e.g. in wall flows (Johnson 1955; Verollet 1969; Verollet & Fulachier 1969; Bremhorst & Bullock 1970; Fulachier 1972) as well as in free flows (Corrsin & Uberoi 1949; Alexopoulos & Keffer 1968; Freymuth & Uberoi 1971, 1973). When the fluctuations are spectrally analysed one finds that the Taylor spectra of u_1' and of θ' are different. In particular, the frequency (wavenumber) range contributing most to the total variance is at a lower frequency for u_1' than for θ'. This consistent difference between the two spectra was found in a jet (Corrsin & Uberoi 1950), in a pipe flow (Bremhorst & Bullock 1970), in a wake (Freymuth & Uberoi 1971) and in a boundary layer (Favre *et al.* 1968; Verollet & Fulachier 1970; Fulachier & Dumas 1971).

As far as predicting the spectra of temperature fluctuations is concerned, the theories of Oboukhov (1949) and Corrsin (1951) were based on similarity considerations in the context of locally isotropic turbulence; they apply only when the wavenumbers are high enough so that the corresponding spectral ranges are independent of the particular conditions of the turbulence generation. In addition, asymptotically high Reynolds numbers are implied. The parameters that are relevant are the dynamical parameters of the velocity transport field, the kinematic viscosity ν and the dissipation ϵ, as well as the thermal diffusivity α and the thermal dissipation ϵ_θ. Analogous forms for the velocity and temperature spectra have been established as shown by, for example, Pao (1965). For the low wavenumber range, which corresponds to the highly energetic and strongly anisotropic part of the fluctuation field, and which strongly depends on the particular conditions in each flow configuration, no theory exists yet. In such a state of affairs, it is necessary to make experiments, especially in the range of the energy-containing eddies, in order to establish, if possible, any analogy that may exist between spectra of velocity and temperature fluctuation fields.

The experiments reported here have been carried out in the turbulent boundary layer, at a relatively low Reynolds number, on a slightly heated plate. In the low frequency (wavenumber) spectral range mentioned above, the experimental results strongly suggest a spectral analogy of a particular form.

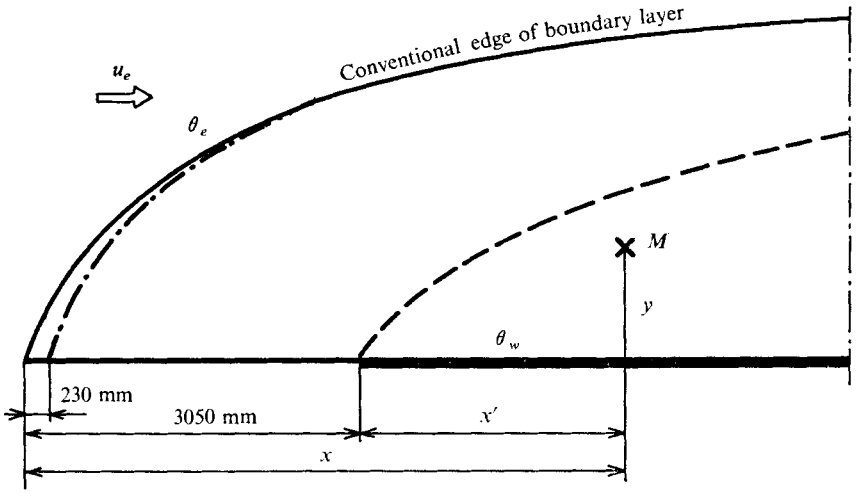

FIGURE 1. Experimental scheme.
Conventional thermal boundary δ_{th}: – – –, case 1; —·—·, case 2.

2. Test facility and experimental procedure

2.1. *Test facility*

Measurements were made in a open-return low-speed wind tunnel driven by a centrifugal blower. Paper and electrostatic dust filters were inserted upstream of the settling chamber. The test section had a $0{\cdot}56 \times 0{\cdot}56$ m square cross-section and was 4·85 m long. The level of the wind-tunnel turbulence at the entrance of the test section was low: the ratio of the r.m.s. velocity fluctuation to the test-section mean velocity u_e was $(\overline{u_1'^2})^{\frac{1}{2}}/u_e \simeq 0{\cdot}0012$. Care was taken to reduce spanwise (three-dimensional) effects in the boundary layer (Favre & Gaviglio 1960) by using special damping screens in the settling chamber. The remaining spanwise variation of the mean velocity inside the boundary layer was about 1% and the maximum variation of the r.m.s. fluctuation $(\overline{u_1'^2})^{\frac{1}{2}}/u_e$ reached $\pm 4\%$ in the outer part of the boundary layer.

The turbulent boundary layer developed on the flat floor of the test section. Because of the low Reynolds number, transition to turbulence was triggered at the entrance of the test section by means of a strip.

Electrical heaters were installed under the floor. The surface temperature was monitored by 121 thermocouples suitably inserted in the wall material. The mean surface temperature varied over the entire plate by less than 4% of the average overheat (Fulachier 1972).

Figure 1 shows the two thermal configurations. For case 1, the beginning of the heated zone was some distance downstream from the transition to turbulence. The thickness δ_{th} of the thermal boundary layer, corresponding to the condition $\overline{\theta} \simeq \theta_e$, was well inside the conventional thickness of the boundary layer. For case 2, the beginning of heating was very near the transition to turbulence and the turbulent flow was completely heated essentially from its beginning. In this

case it was possible to distinguish the turbulent flow from the outer potential flow by using the temperature of the fluid as an intermittency criterion $\theta > \theta_e$ in the turbulent zone and $\theta \simeq \theta_e$ in potential flow, as shown experimentally in the boundary layer by Dumas, Fulachier & Arzoumanian (1972). The method, now classic, is used even in free flows, where the rate of entrainment of potential flow is higher than in the boundary layer (Kovasznay & Ali 1974; Antonia 1974).

2.2. *Mean flow characteristics of the heated boundary layer*

At the measurement station ($x = 3{\cdot}69$ m), the mean flow characteristics were

outer free-stream velocity	$u_e = 12$ m s^{-1},
conventional boundary-layer thickness	$\delta = 62$ mm $\quad (\bar{u}_1 = u_e)$,
displacement thickness	$\delta_1 = 8{\cdot}13$ mm,
skin-friction velocity	$u_* = 48$ cm s^{-1},
skin-friction coefficient	$c_f = 32 \times 10^{-4}$.

Owing to limitations of the available equipment, the Reynolds number was rather low, $\mathscr{R}_\delta \simeq 50000$, and the streamwise pressure gradient was slightly negative; the absolute value of the Clauser parameter $\pi = \delta_1 \rho^{-1} u_*^{-2} d\bar{p}/dx$ was small ($|\pi| \leqslant 0{\cdot}019$).

In case 1, the mean thermal conditions were

$$\theta_w - \theta_e = 21\ ^\circ\text{C} \quad \text{with} \quad \delta_{\text{th}} \simeq 0{\cdot}52\delta,$$

the Stanton number being $St = 20{\cdot}5 \times 10^{-4}$ and the corresponding friction temperature being $\theta_* = 1{\cdot}2\ ^\circ$C.† In case 2,

$$\theta_w - \theta_e = 22\ ^\circ\text{C}, \quad \delta_{\text{th}} \simeq \delta, \quad St = 16{\cdot}7 \times 10^{-4}, \quad \theta_* = 0{\cdot}99\ ^\circ\text{C}.$$

The influence of such a low heating on the profiles of mean velocity, variance and covariance was not detectable, indicating that the buoyancy effects were negligible within the accuracy of the measurements.

2.3. *Experimental procedure*

The measurements were made with constant-current hot-wire anemometers. The wire, made of platinium–rhodium, was generally $2{\cdot}5\ \mu$m in diameter and $0{\cdot}8$ mm in length. The hot-wire thermal lag, less than $0{\cdot}4 \times 10^{-3}$ s, was always compensated by an analog circuit and the proper adjustment was obtained by using a high frequency square-wave method (Gaviglio 1962). The distance separating the planes of the two wires of an X-probe was chosen as 0·3–0·4 mm so as to be large enough to avoid the mutual interaction of the two wires but not too large with respect to spatial gradients to be encountered. Indeed, it was noticed that the correlation between the temperature fluctuations θ' measured by the two wires vanishes rapidly with increasing separation distance; this holds equally well for u_2' and u_3'.

The variance and the covariance of temperature and velocity-component

† $St = q_w/\rho_e c_p u_e(\theta_w - \theta_e)$, $\theta_* = q_w/\rho_w c_p u_*$, q_w = heat flux at the wall.

fluctuations have been obtained by the 'fluctuation-diagram' method. This was first established for supersonic flows (Kovasznay 1953), but may be applied, as here, to low velocity heated flow as shown by Verollet (1969, 1972). The method will be recalled below, for the case of frequency-filtered fluctuations. Measurements of $\overline{u_1'^2}$, $\overline{\theta'^2}$ and $\overline{\theta' u_1'}$ were also made by using two parallel wires and the variables u_1' and θ' were separated using an analog device, but with that method the accuracy was less than that obtained by the fluctuation-diagram method.

Measurements of spectra. The properly compensated hot-wire output signals were passed through a frequency filter, in fact an analog analyser (Dumas 1964). The central frequency range of the analyser extended from 1 Hz to 6000 Hz; above 3000 Hz it was necessary to apply some corrections in order to take into account the effect of the high energy level at lower frequencies (diaphonic effect). Further corrections were made for the anemometer band-pass characteristics (1–6000 Hz at 3 dB).

The method used to measure the cospectra, and also in some cases the temperature spectra, was based on the above-mentioned fluctuation-diagram method. Using a caret to denote a frequency-filtered fluctuation, the usual linearized theory gives for the hot-wire output voltage

$$\hat{e}'(t) = -\gamma \hat{u}_1'(t)/\bar{u}_1 + \beta \hat{\theta}'(t)/\bar{\theta}, \tag{1}$$

where γ and β are sensitivity coefficients. From (1) we obtain the statistical equation by squaring and averaging:

$$\frac{\overline{(\hat{e}')^2}}{\beta^2} = s^2 \frac{\overline{(\hat{u}_1')^2}}{(\bar{u}_1)^2} - 2s \frac{\overline{\hat{u}_1' \hat{\theta}'}}{\bar{u}_1 \bar{\theta}} + \frac{\overline{(\hat{\theta}')^2}}{(\bar{\theta})^2} \quad \text{with} \quad s = \frac{\gamma}{\beta}. \tag{2}$$

This is a hyperbolic relationship between $[\overline{(\hat{e}')^2}]^{\frac{1}{2}}/\beta$ and s in which the variances $\overline{(\hat{u}_1')^2}$ and $\overline{(\hat{\theta}')^2}$ and covariance $\overline{\hat{u}_1' \hat{\theta}'}$ are constant parameters.

For zero heating current, the variable s is zero, and it increases monotonically with increasing heating current. By using several (e.g. twelve) values of the heating current, it is possible to obtain the hyperbola with good accuracy. Hence the variances and covariance can be calculated from the parameters of the hyperbola.

When using a filter of a narrow bandwidth Δf, (2) becomes, to a good approximation, a relationship among the spectra:

$$\frac{\overline{e'^2}}{\beta^2} F_e(f)\,\Delta f = s^2 \frac{\overline{u_1'^2}}{(\bar{u}_1)^2} F_1(f)\,\Delta f - 2s \frac{\overline{u_1' \theta'}}{\bar{u}_1 \bar{\theta}} P_{1,\theta}(f)\,\Delta f + \frac{\overline{\theta'^2}}{(\bar{\theta})^2} F_\theta(f)\,\Delta f, \tag{3}$$

where $F_1(f)$, $F_\theta(f)$ and $P_{1,\theta}(f)$ are respectively the Taylor spectra and cospectrum, normalized to unity, of the u_1' and θ' fluctuations, and $F_e(f)$ is the conventional power spectrum of the output voltage signal. In fact, the analyser used had a bandwidth which was not constant, but proportional to the centre-frequency; this is the reason why figure 2 shows examples of the quantity $[\overline{e'^2}\beta^{-2} f F_e(f)]^{\frac{1}{2}}$ for two different frequencies, plotted on an arbitrary scale, as a function of the sensitivity ratio $s' = s\bar{\theta}/(\theta_w - \bar{\theta})$. The curves are really portions of hyperbolae

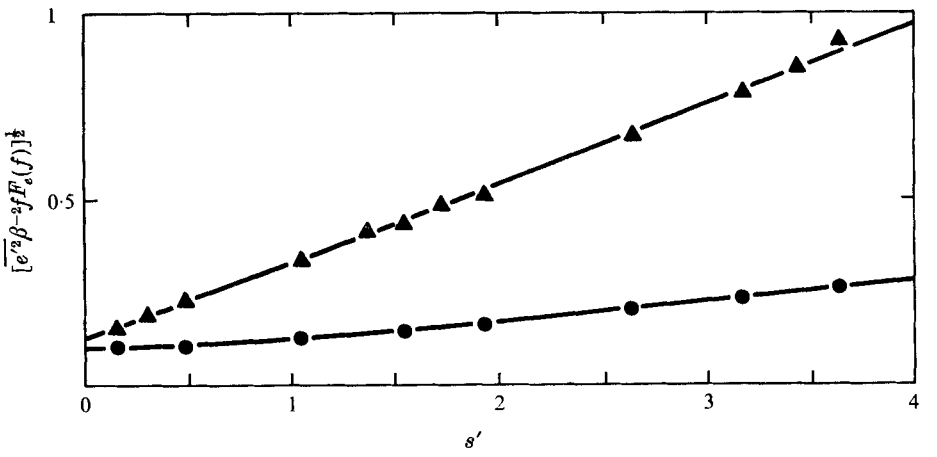

FIGURE 2. Fluctuation diagram of the filtered signals (single wire); $y/\delta = 0{\cdot}113$, case 1. ▲, $f = 61{\cdot}2$ Hz; ●, $f = 2599$ Hz.

fitted to the data. Each curve yields, for a given frequency f, the corresponding values of three quantities: the spectra $F_1(f)$ and $F_\theta(f)$ and cospectrum $P_{1,\theta}(f)$, each multiplied by an arbitrary constant.

The temperature fluctuation spectra $F_\theta(f)$ may be obtained, as usual, more directly by using a hot wire with a very low heating current. However, when using (3) it was necessary to apply some corrections, mainly due to the first-order term with respect to s, i.e. $-2s(\overline{u_1'\theta'}/\bar{u}_1\bar{\theta})\,P_{1,\theta}(f)$, which was not negligible under the existing operating conditions; this term, which is often ignored, can be the principal source of errors in measurements of temperature fluctuations, even when using relatively low heating currents.

In order to measure the cospectrum $P_{2,\theta}$ of the fluctuations in the velocity component u_2' normal to the wall and the temperature, it was necessary to use an X-wire probe. The fluctuation-diagram method applies in a similar way:

$$\frac{\overline{(\hat{e}')_{\mathrm{I}}^2}-\overline{(\hat{e}')_{\mathrm{II}}^2}}{4\varepsilon\beta} = -s\frac{\overline{\hat{u}_1'\hat{u}_2'}}{\bar{u}_1^2}+\frac{\overline{\hat{u}_2'\hat{\theta}'}}{\bar{u}_1\bar{\theta}}, \tag{4}$$

where $(\hat{e}')_{\mathrm{I}}$ and $(\hat{e}')_{\mathrm{II}}$ are the outputs of the two wires of the X-probe; ε and β are the sensitivity coefficients, corresponding respectively to the orthogonal velocity and temperature of the X-probe. In this case, the variable

$$[\overline{(\hat{e}')_{\mathrm{I}}^2}-\overline{(\hat{e}')_{\mathrm{II}}^2}]/4\varepsilon\beta$$

was a linear function of s, which determines the cospectra $\overline{\hat{u}_1'\hat{u}_2'}$ and $\overline{\hat{u}_2'\hat{\theta}'}$ or $P_{1,2}$ and $P_{2,\theta}$, respectively. Equation (4) reads in spectral form, with the same assumptions as for (3),

$$\frac{\overline{(e')_{\mathrm{I}}^2}F_{e\mathrm{I}}(f)-\overline{(e')_{\mathrm{II}}^2}F_{e\mathrm{II}}(f)}{4\varepsilon\beta}\Delta f = -s\frac{\overline{u_1'u_2'}}{\bar{u}_1^2}P_{1,2}(f)\,\Delta f+\frac{\overline{u_2'\theta'}}{\bar{u}_1\bar{\theta}}P_{2,\theta}(f)\,\Delta f. \tag{5}$$

Figure 3 shows diagrams giving $[\overline{(e')_{\mathrm{I}}^2}F_{e\mathrm{I}}(f)-\overline{(e')_{\mathrm{II}}^2}F_{e\mathrm{II}}(f)]f/4\varepsilon\beta$ as a function

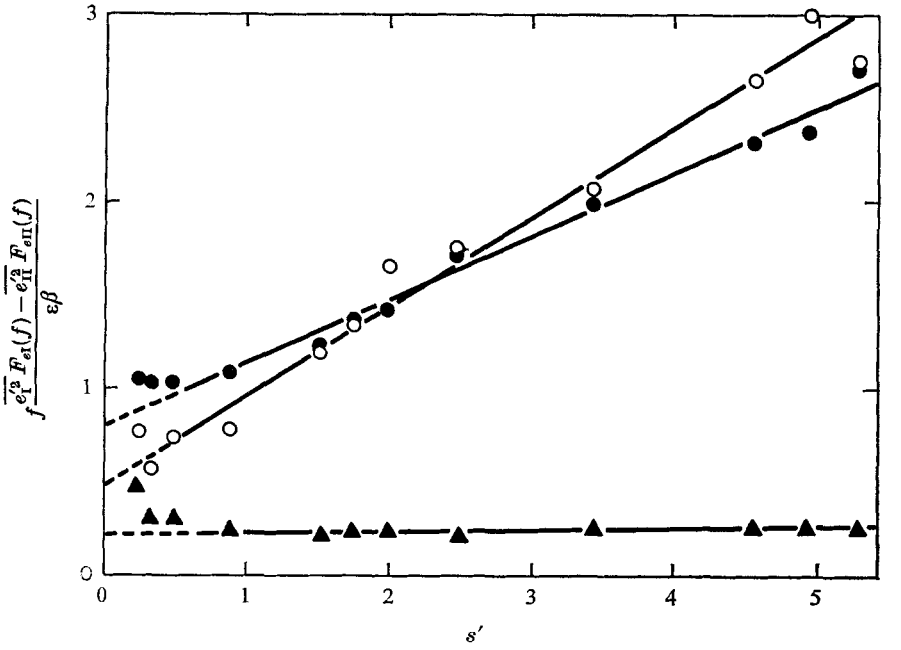

FIGURE 3. Fluctuation diagram of the filtered signals (X-wires); $y/\delta = 0{\cdot}113$, case 2. ○, $f = 25{\cdot}6$ Hz; ●, $f = 634$ Hz; ▲, $f = 1983$ Hz.

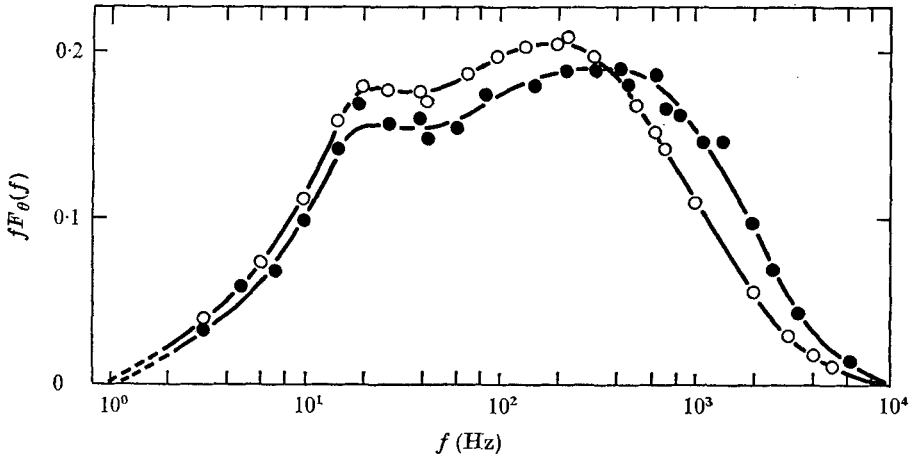

FIGURE 4. Influence of the time compensation of the wire; $y_* = 80$. ●, correct time constant, $M = 253$ μs; ○, under compensated, $M' = 0{\cdot}67M$.

of s' plotted on an arbitrary scale, for three frequencies. Each straight line gives, for a frequency f, the corresponding values of the cospectra $P_{1,2}$ and $P_{2,\theta}$ multiplied by arbitrary constants. In fact, in drawing the straight lines no account was taken of the data corresponding to the weakest heating current. Although a full error analysis was not made, it was noticed that the Reynolds-stress cospectra $P_{1,2}$ measured both without heating and in a heated flow were practically the same (Fulachier 1972; see also figure 11).

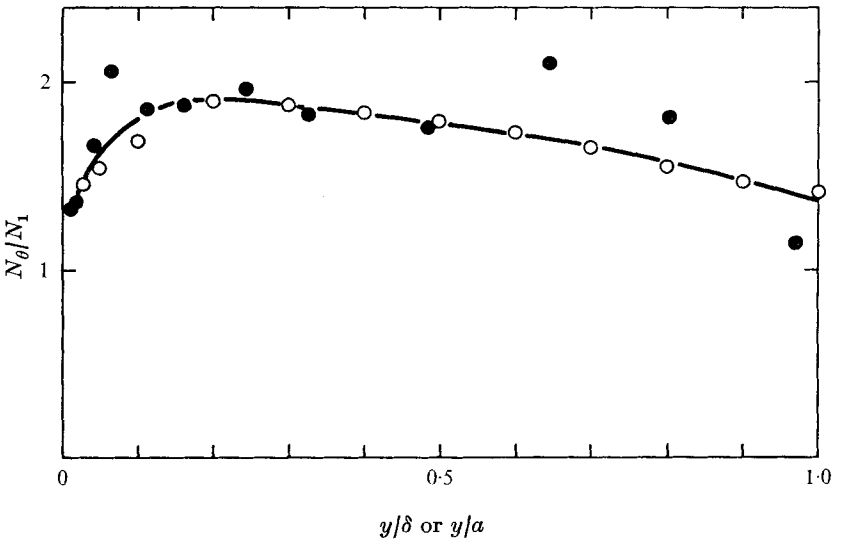

FIGURE 5. Dissipation frequency ratio N_θ/N_1 in a boundary layer and in a pipe. ●, boundary layer (case 2); ○, pipe (a = radius of pipe).

In the figures, the spectra are weighted with frequency in the form $fF(f)$ and plotted as a function of $\log f$. In this presentation, the area under the curve is proportional to the variance, a very useful feature for our purpose here.

An important effect due to the thermal lag compensation was noticed. Figure 4 shows the error introduced in the spectral density distribution owing to incorrect compensation of the hot wire (33% undercompensated).

Although the primary interest in the present investigation was in the energy-containing eddies, a check on the measurements in the dissipation spectral range has been made. For this purpose it is assumed that the ratio of the dissipation frequencies N_θ/N_1 is the same in the wall region of both the boundary layer and the pipe flow. The dissipation frequency is defined by

$$N_\xi^2 = \int_0^\infty f^2 F(f)\, df = \frac{1}{4\pi^2}\overline{\left(\frac{\partial \xi}{\partial t}\right)^2} \Big/ \overline{\xi^2},$$

where N_θ and N_1 correspond to θ' and u_1' respectively.

Figure 5 shows satisfactory agreement, even outside of the wall region, between the values of N_θ/N_1 measured in the boundary layer by the spectral method and those measured recently in pipe flow by Elena (1975), using an analog derivative device and a hot wire 1 μm in diameter, with very low overheating.

3. Experimental results

Although the spectra were obtained as functions of the frequency, for convenience, as usual, the wavenumber $k_1 = 2\pi f/\bar{u}_1$ will be used. This change, however, must be considered only as a change of scale without any physical

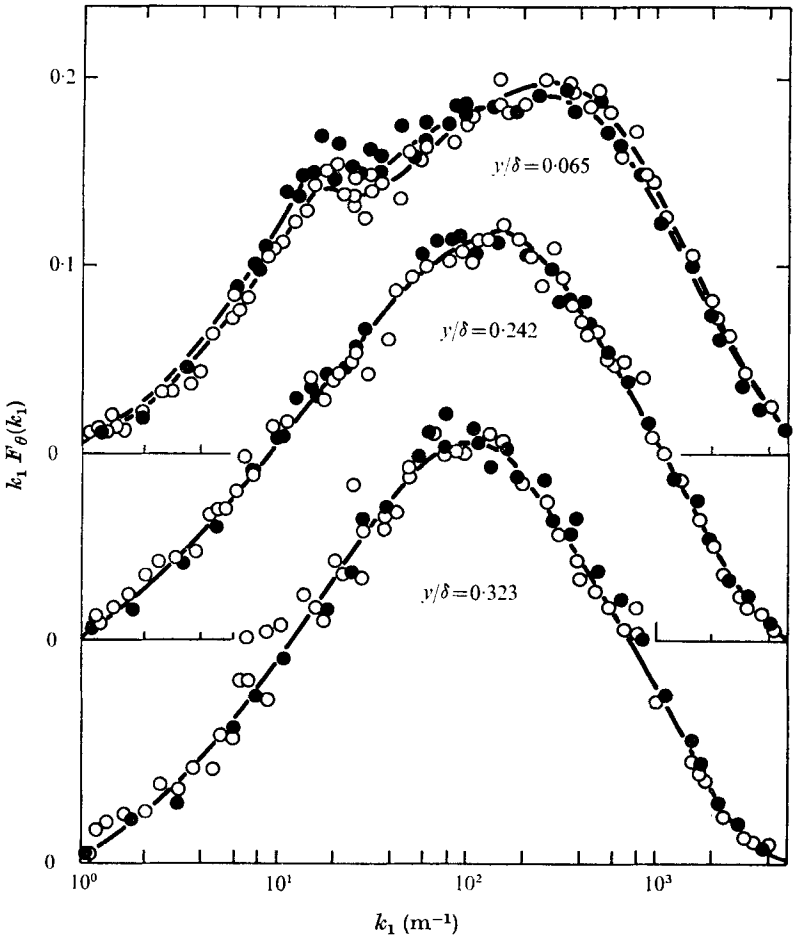

FIGURE 6. Comparison of temperature spectra in the two experimental cases; $x = 3{\cdot}69$ m. ○, case 1, $\delta_{th} \simeq 0{\cdot}52\delta$; ●, case 2, $\delta_{th} \simeq \delta$.

implications. Moreover, the purpose of this research is to compare velocity and temperature spectra at the same point in space, therefore the numerical value of the mean velocity $\bar{u}_1$ is irrelevant.

3.1. *Influence of thermal boundary conditions on temperature spectra*

Figure 6 compares temperature spectra $F_\theta(k_1)$ measured for the two different heating configurations (cases 1 and 2) taken at the longitudinal distance $x = 3{\cdot}69$ m at three distances from the wall: $y/\delta = 0{\cdot}065$, $y/\delta = 0{\cdot}242$ and $y/\delta = 0{\cdot}323$. It must be stressed that cases 1 and 2 correspond to very different thermal boundary conditions, while the dynamic configuration of the boundary layer remained unchanged (for case 1, $y/\delta_{th} \simeq 0{\cdot}52y/\delta$, and for case 2, $y/\delta_{th} \simeq y/\delta$). The difference between measured spectra in the two cases is very small indeed even as far as $y/\delta = 0{\cdot}323$. So, at these distances from the wall, the different thermal boundary conditions had no significant effect on the spectra. On the

other hand, the mean temperature profiles in the two cases, properly scaled with θ_* and u_*, are similar up to only about $y/\delta \simeq 0{\cdot}16$.

From here on, the experimental conditions in case 1 apply to data given in figures 7 (*a*) and (*b*) and the conditions in case 2 to all the other figures.

3.2. *A comparison between velocity and temperature spectra and cospectra*

As was stated earlier, in general the fluctuations θ' are strongly correlated with the longitudinal velocity component u_1' and also with the normal component u_2'. Indeed, $r_{1,\theta}$, the correlation coefficient between u_1' and θ', is negative in the present case, with an absolute value of about 0·9 at the outer edge of the viscous sublayer ($y_* = u_* y/\nu \sim 10$), gradually dropping to about 0·5 in the central part of the boundary layer; in the intermittent zone, it decreases practically to zero. Near the wall, Elena (1975) has found, in a pipe, the absolute value of $r_{1,\theta}$ in the viscous sublayer to decrease rapidly towards the wall. In the boundary layer, $r_{2,\theta}$, the correlation coefficient between u_2' and θ', remains practically constant, at about 0·6, in the fully turbulent portion. It decreases rapidly in the intermittent region. These results were obtained in case 2, with the entire turbulent region heated (Fulachier 1972).

Systematic measurements were made to obtain spectra of θ' and u_1', as well as cospectra of θ' and u_1', at several positions in the boundary layer (Fulachier 1972), and some typical examples are shown here. Figure 7 (*a*) shows the weighted cospectrum $-r_{1,\theta}P_{1,\theta}(k_1)$ obtained in case 1, together with the velocity and temperature spectra $F_1(k_1)$ and $F_\theta(k_1)$ respectively. The distance from the wall is $y/\delta = 0{\cdot}113$, i.e. $y_* = 224$; the value of $r_{1,\theta}$ is $-0{\cdot}64$. The temperature spectrum F_θ has been corrected for velocity contamination (see §2.3). It is clear that F_θ is markedly different from the velocity spectrum F_1 except for lower frequencies. Moreover, there is a flat part and an inflexion point in the F_θ curve in

$$15 \text{ m}^{-1} < k_1 < 30 \text{ m}^{-1},$$

corresponding to the flat portion of the F_1 curve and to where the cospectrum $P_{1,\theta}$ is also near its maximum value. However, the variation suggested by Tchen (k_1^{-1}) applies to a smaller spectral range for temperature than for longitudinal velocity. Figure 8 (*a*), which gives the spectrum $F_2(k_1)$ of the normal velocity component, the temperature spectrum $F_\theta(k_1)$ and the cospectrum $r_{2,\theta}P_{2,\theta}(k_1)$ obtained at the same distance from the wall but for case 2, shows that, in the frequency range where F_θ attains its maximum value, F_2 and F_θ are strongly similar.

Figures 7 (*b*) and 8 (*b*) show the same comparison between spectra and cospectra but at a greater distance from the wall ($y/\delta = 0{\cdot}242$, i.e. $y_* = 480$).

From the above results, it appears that the temperature fluctuations are controlled by the streamwise velocity component u_1' at low frequencies but by the normal component u_2' at higher frequencies (Fulachier 1971).

3.3. *Proposed spectral analogy*

The influence of the longitudinal and orthogonal velocity components on the temperature fluctuations has already been demonstrated. With regard to the spanwise component u_3', we note that the correlation $\overline{u_3'\theta'}$ must vanish by virtue

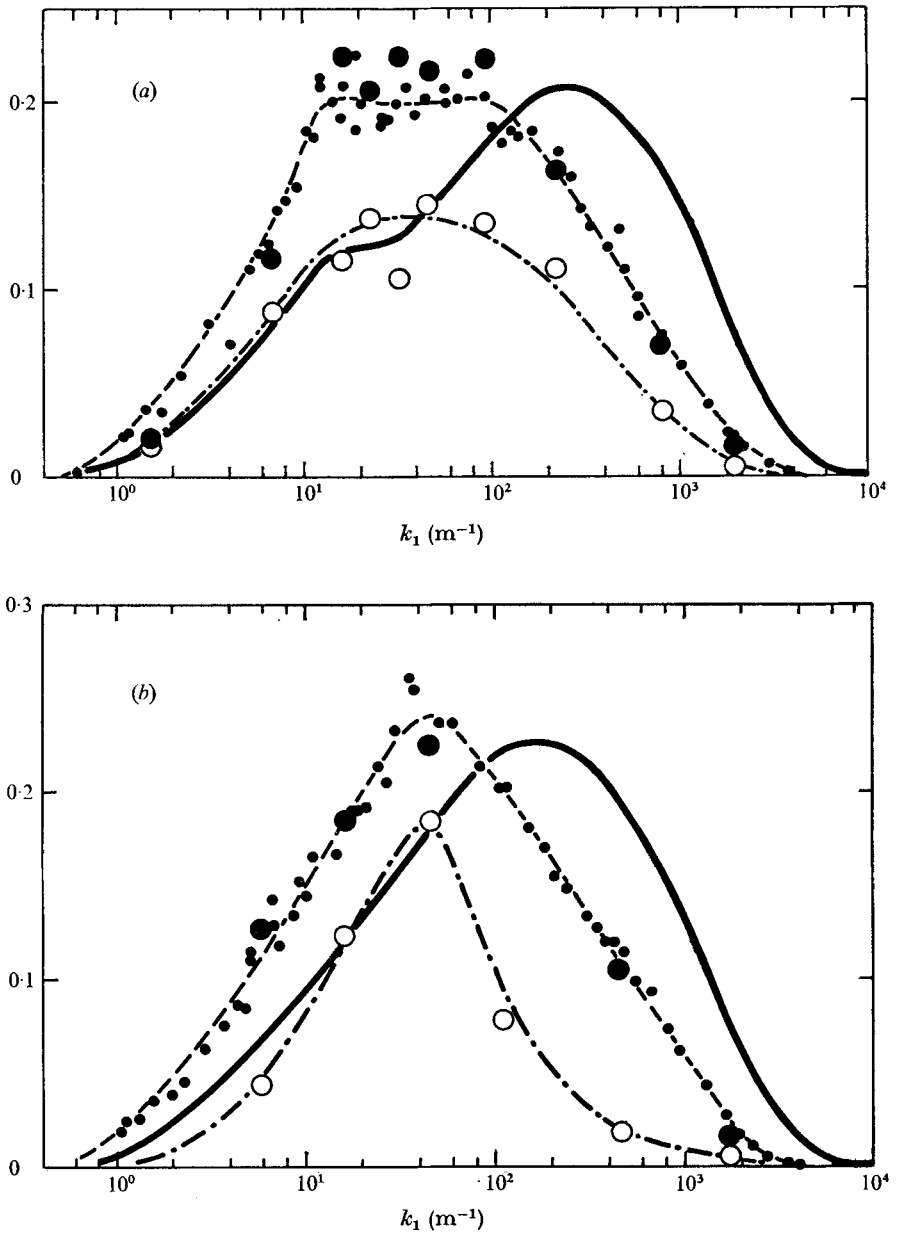

FIGURE 7. Comparison between temperature spectrum and longitudinal velocity spectrum; case 1. ——, $k_1 F_\theta$; ●, $k_1 F_1$, heated flow; ●, $k_1 F_1$, isothermal flow; ○, cospectrum, $-k_1 r_{1,\theta} P_{1,\theta}$. (*a*) $y_* = 224$, $r_{1,\theta} = -0{\cdot}64$. (*b*) $y_* = 480$, $r_{1,\theta} = -0{\cdot}48$.

of symmetry when the mean flow is two-dimensional. However, because the temperature field is essentially dependent upon the velocity field, there are instantaneous lateral heat fluxes. Therefore, the three velocity components contribute to the transfer of heat, when the latter is considered as a passive scalar contaminant. If we then consider the corresponding spectra, the temperature

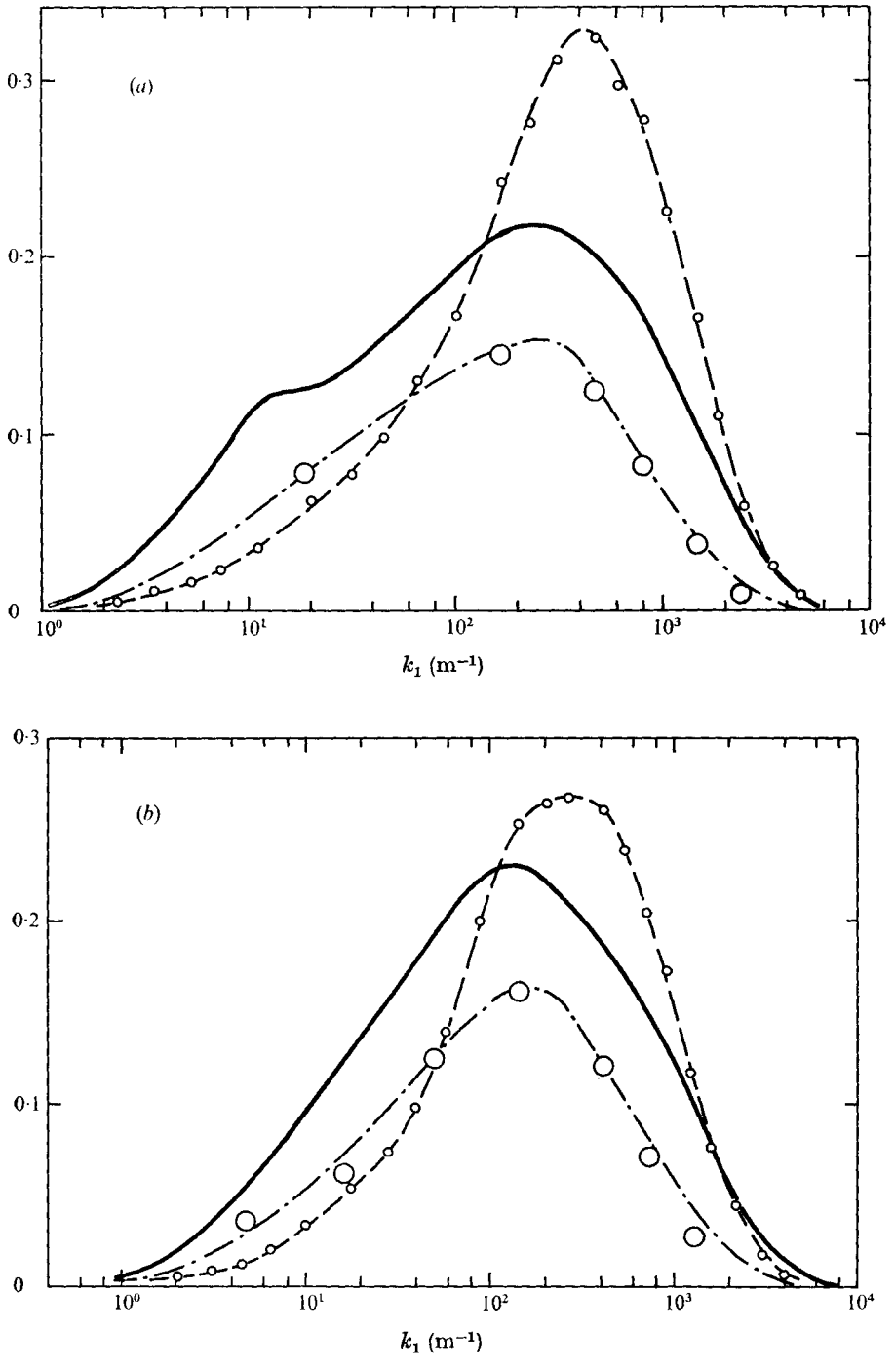

FIGURE 8. Comparison between temperature spectrum and orthogonal velocity spectrum. ——, $k_1 F_\theta$; ○, $k_1 F_2$, isothermal flow; ○, cospectrum, $k_1 r_{2,\theta} P_{2,\theta}$ ($r_{2,\theta} = 0{\cdot}60$). (*a*) $y_* = 224$. (*b*) $y_* = 480$.

fluctuations and the three components of the fluctuating velocity vector may be linked, though the $\overline{u_3'\theta'}$ correlation is zero. Indeed one may recall that, for isotropic turbulence, $\overline{u_i'u_j'}$ is zero for $i \neq j$. However there exists an explicit relationship, for incompressible flow, between the spectra of the u_i' and u_j' components.

In the spirit of the above remarks, which leave the problem open, we have searched empirically for a spectral analogy between the temperature fluctuations and an appropriate scalar involving all three components of the velocity fluctuations. The first step (Fulachier & Dumas 1971; Fulachier 1972), for the variances, is to compare the autocorrelation $\overline{\theta'(t)\,\theta'(t+\tau)}$ and the scalar autocorrelation of the velocity vector defined by $\overline{\mathbf{v}'(t).\mathbf{v}'(t+\tau)}$, where τ is the time lag and $\mathbf{v}'$ the velocity vector, with components u_1', u_2' and u_3'.

If we introduce the Fourier transforms of the above autocorrelations, the temperature spectrum $F_\theta(f)$ and the vector velocity power spectrum $Q(f)$ must be compared. The latter is defined as

$$Q(f) = \frac{\overline{u_1'^2}}{\overline{q'^2}}F_1(f) + \frac{\overline{u_2'^2}}{\overline{q'^2}}F_2(f) + \frac{\overline{u_3'^2}}{\overline{q'^2}}F_3(f), \tag{6}$$

with

$$\overline{q'^2} = \overline{u_1'^2} + \overline{u_2'^2} + \overline{u_3'^2}.$$

The proposed analogy was tested and figures 9 and 10 compare the temperature spectrum $k_1F_\theta(k_1)$ with each of the three velocity-component spectra

$$\frac{\overline{u_1'^2}}{\overline{q'^2}}k_1F_1(k_1), \quad \frac{\overline{u_2'^2}}{\overline{q'^2}}k_1F_2(k_1), \quad \frac{\overline{u_3'^2}}{\overline{q'^2}}k_1F_3(k_1),$$

as well as with the newly defined spectrum $k_1Q_1(k_1)$, all plotted as function of $\log k_1$ at various distances from the wall.

Figure 9(*a*) displays results obtained at $y_* = 16$, very close to the region of the maximum production of turbulent kinetic energy. F_2 and F_3 were measured only at some distance from the wall ($y_* \geqslant 80$). It was assumed that near the wall the non-dimensional form of these spectra is independent of y_* as long as they are presented as functions of the wavenumber k_1 (and not of the frequency f). The mean-square values $\overline{u_2'^2}$ and $\overline{u_3'^2}$ were necessary for the weighting factors; they were borrowed from Klebanoff (1954). In fact, $\overline{u_2'^2}/\overline{q'^2} \simeq 0{\cdot}04$ and $\overline{u_3'^2}/\overline{q'^2} \simeq 0{\cdot}14$, and consequently the error introduced by the estimation of the spectra in the above-described manner had no great influence on the spectrum $Q(k_1)$ in the region where it depends mainly on the longitudinal spectrum $F_1(k_1)$, which contributes 82%. For this reason, at $y_* = 16$, F_1 and Q are not much different. The temperature spectrum F_θ is also similar, but lies still closer to Q. Note that in this figure the temperature spectrum was not corrected for velocity contamination but, when taking into account the fact that the absolute value of the correlation coefficient between θ' and u_1' is high for the energy-containing frequencies, the eventual correction would be small and it would only slightly shift the temperature spectrum towards the higher frequencies.

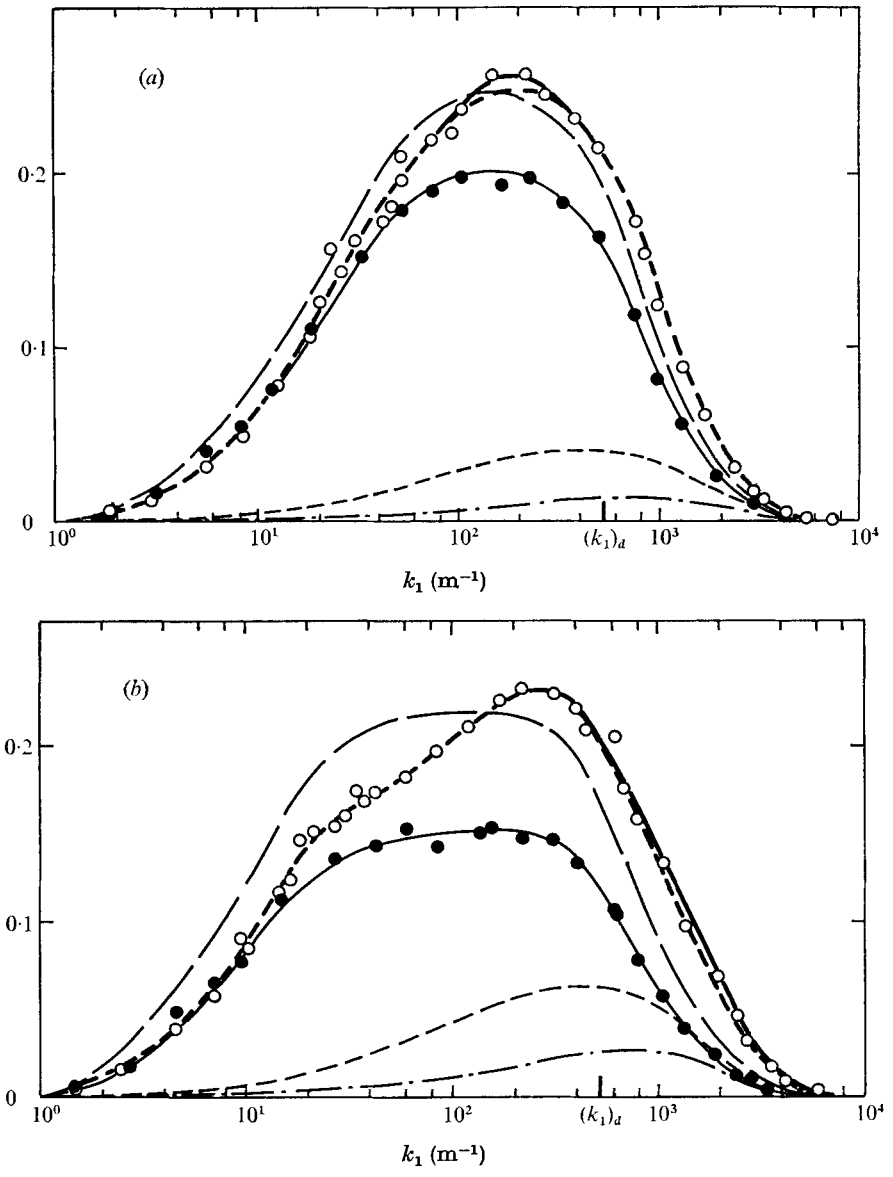

FIGURE 9. Comparison between temperature spectrum and velocity spectrum Q. ○, $k_1 F_\theta$, measured; ——, $k_1 Q$; — —, $k_1 F_1$; ●, $(\overline{u_1'^2}/\overline{q'^2})\, k_1 F_1$; —·—, $(\overline{u_2'^2}/\overline{q'^2})\, k_1 F_2$; – – – –, $(\overline{u_3'^2}/\overline{q'^2})\, k_1 F_3$. (*a*) $y_* = 16$. (*b*) $y_* = 32$.

Figure 9(*b*) shows spectra obtained in the same manner, using the same type of estimates as in the previous figure, but now at the distance $y_* = 32$. It may be noticed that the temperature spectrum F_θ appears to be very close to Q but differs markedly from F_1. This is explained by the relative decrease in the variance of the longitudinal component of the velocity fluctuation with respect to that of the other components.

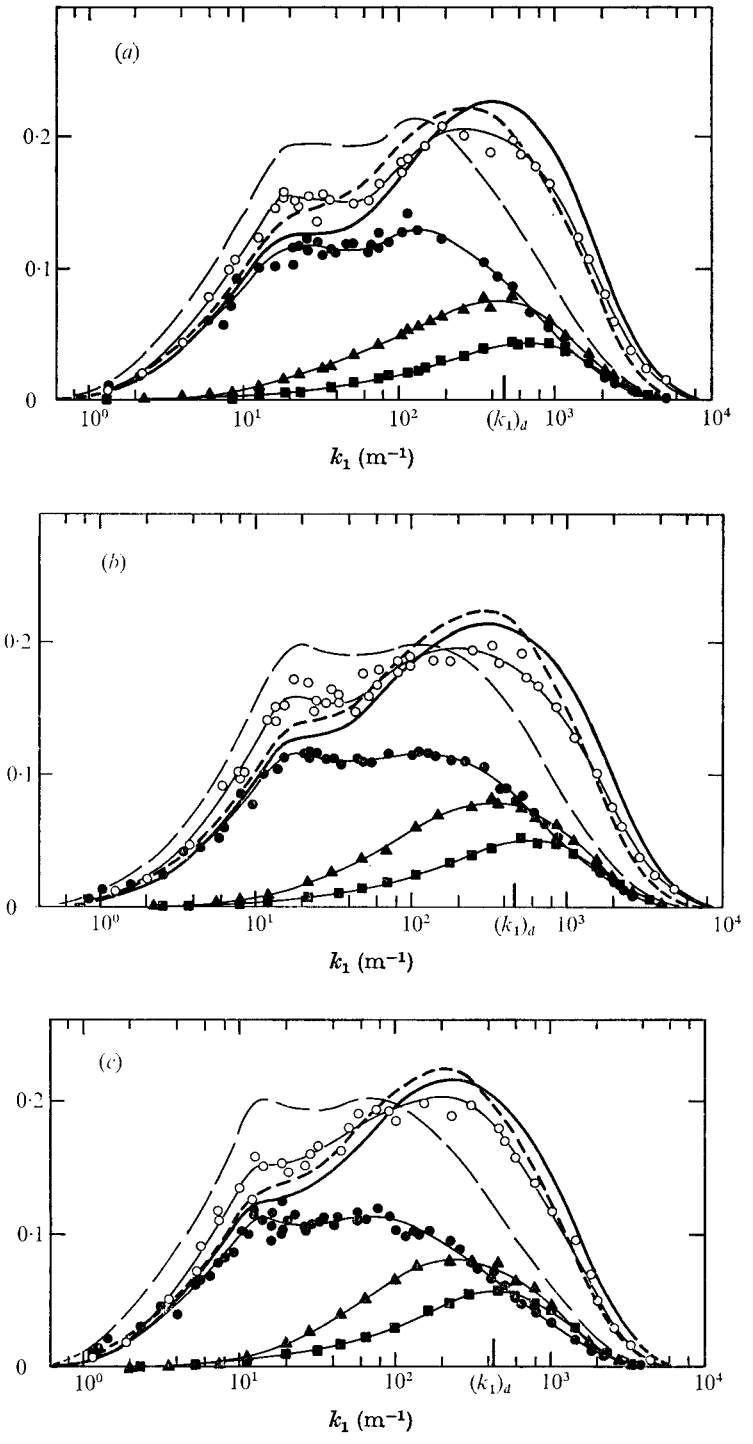

FIGURES 10 (*a–c*). For caption see page 273.

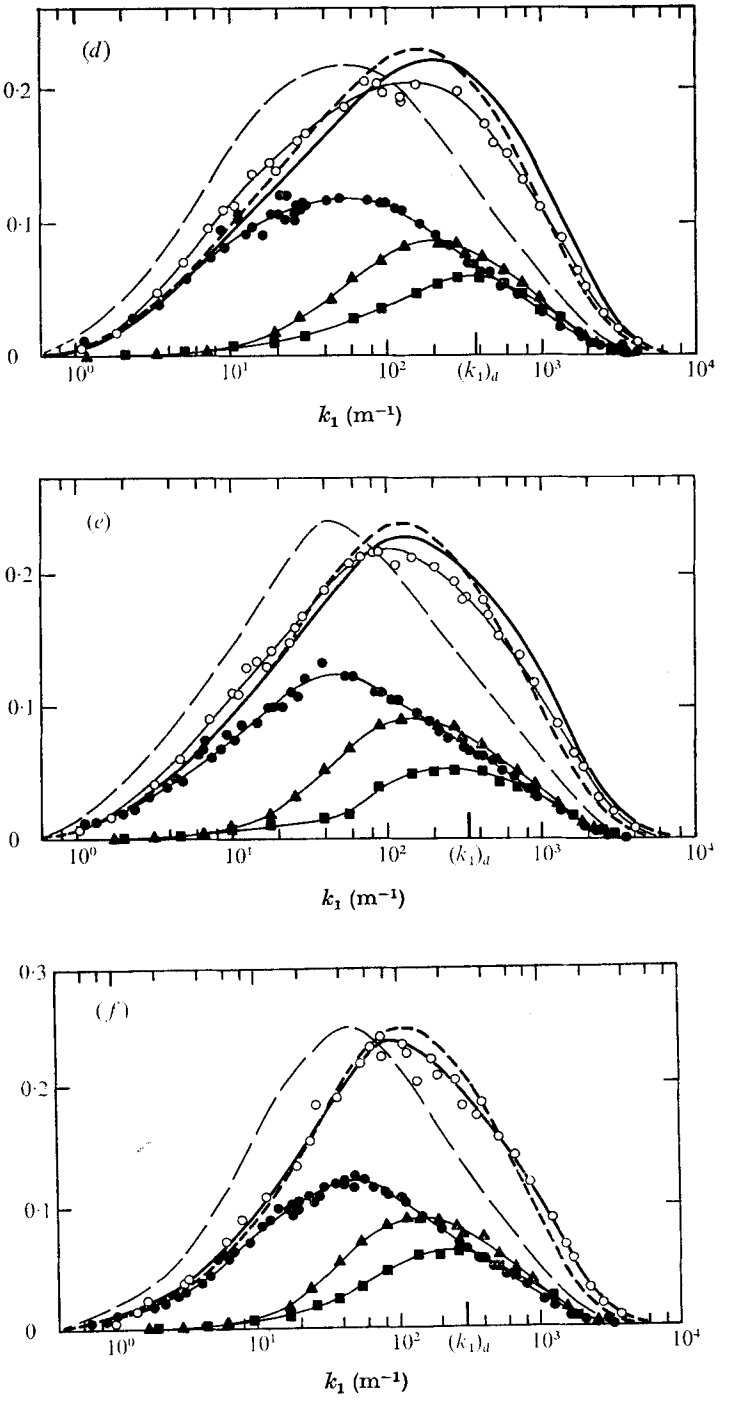

FIGURES 10 (*d–f*). For caption see page 273.

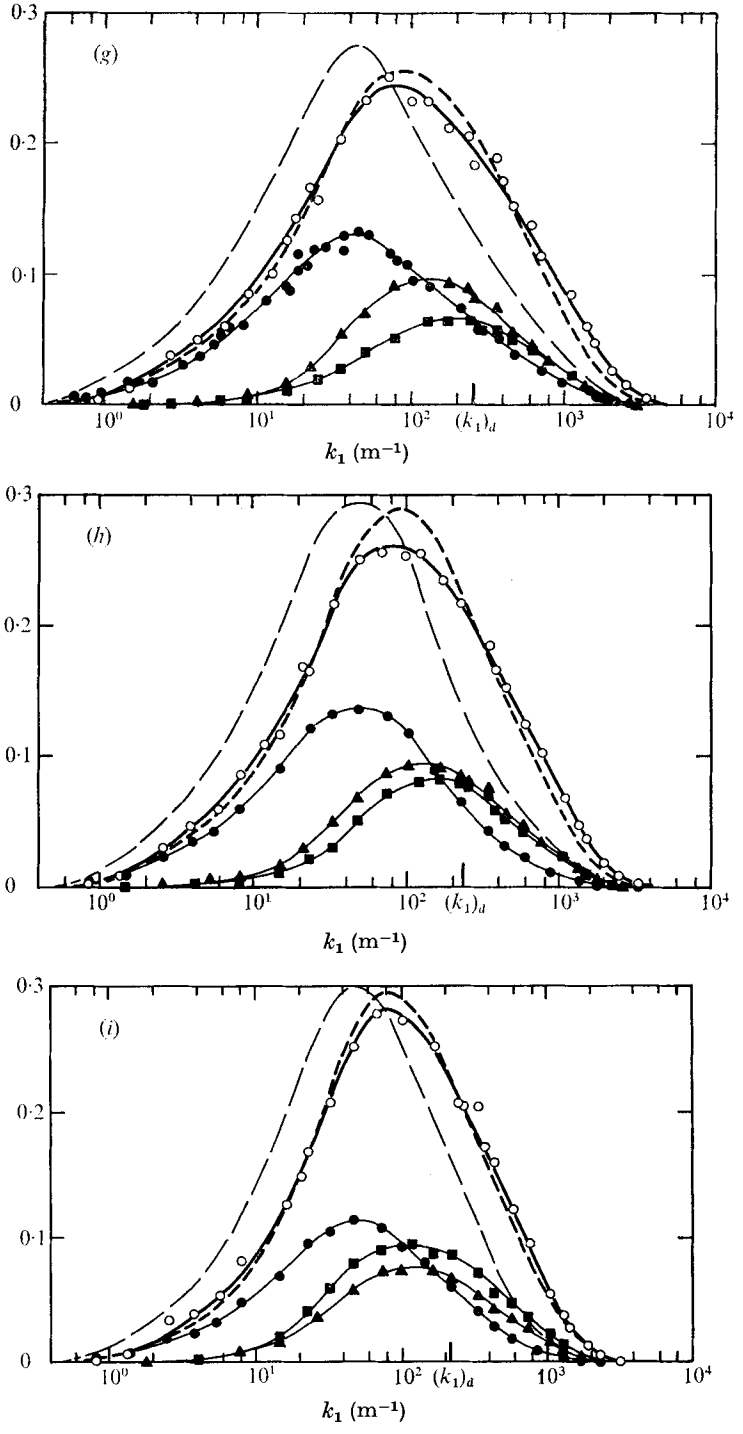

FIGURE 10. Comparison between temperature spectrum and velocity spectrum Q. ○, $k_1 F_\theta$, measured; ——, $k_1 F_\theta$, corrected; — —, $k_1 Q$; — —, $k_1 F_1$; ●, $(\overline{u_1'^2}/\overline{q'^2})\, k_1 F_1$; ■, $(\overline{u_2'^2}/\overline{q'^2})\, k_1 F_2$; ▲, $(\overline{u_3'^2}/\overline{q'^2})\, k_1 F_3$. (*a*) $y_* = 80$. (*b*) $y_* = 128$. (*c*) $y_* = 224$. (*d*) $y/\delta = 0{\cdot}161$ ($y_* = 320$). (*e*) $y/\delta = 0{\cdot}242$. (*f*) $y/\delta = 0{\cdot}323$. (*g*) $y/\delta = 0{\cdot}484$. (*h*) $y/\delta = 0{\cdot}645$. (*i*) $y/\delta = 0{\cdot}806$.

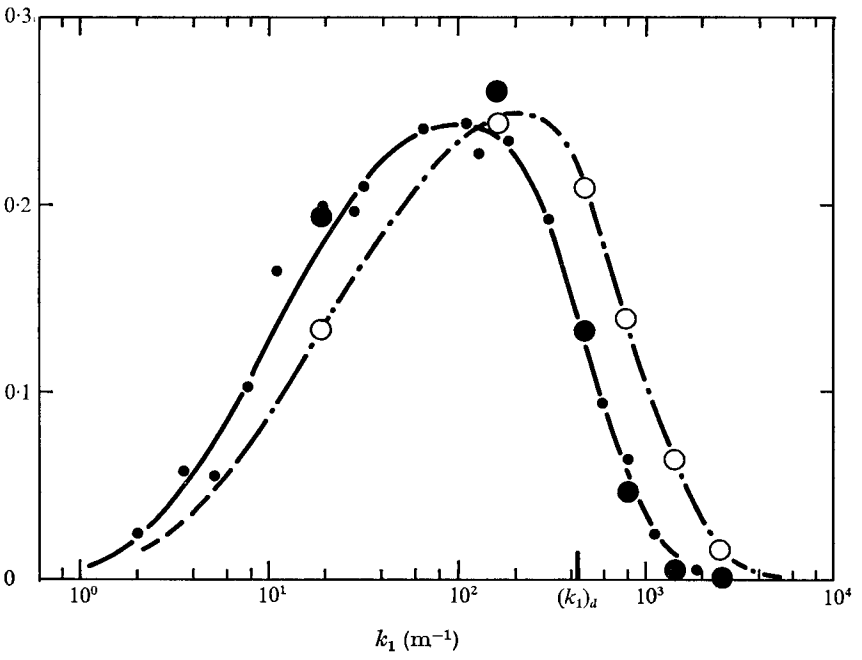

FIGURE 11. Temperature and velocity turbulent production cospectra; $y_* = 224$. ●, $k_1 P_{1,2}$, isothermal flow; ●, $k_1 P_{1,2}$, heated flow; ○, $k_1 P_{2,\theta}$.

In figures 10(*a*), (*b*) and (*c*) similar data are shown for distances $y_* = 80$, 128 and 224 respectively, which still correspond to the inner part of the boundary layer. Here the temperature spectra were corrected for the effect of contamination by the longitudinal velocity component. In this region ($80 < y_* < 224$), the temperature and longitudinal velocity spectra differ more than they do nearer to the wall because the longitudinal-component variance has decreased with respect to the others. On the other hand, the temperature spectra are quite close to the Q spectra for all but the highest frequencies. A flat part appears in the $k_1 F_1$ spectrum (k_1^{-1} variation according to Tchen's law) and, over a more narrow frequency range, in the $k_1 Q$ and $k_1 F_\theta$ spectra, as previously noted.

Figures 10(*d*)–(*i*) show the spectra in the outer part of the boundary layer at $y/\delta = 0{\cdot}161$ ($y_* = 320$), 0·242, 0·323, 0·484, 0·645 and 0·806 respectively. Corrections for velocity contamination in the temperature spectra were made only in figures 10(*d*) and (*e*). The spectra Q and F_θ almost coincide except at the highest frequencies. The streamwise velocity spectrum F_1 is always quite different from F_θ, although in the intermittent region this is less visible. The spectral variation with k_1^{-1} disappears for F_1 and, consequently, according to the analogy, for the Q and F_θ spectra.

So it was found that, at this Reynolds number, the proposed analogy applies in all parts of the boundary layer for the lowest frequencies, which include about 80% of contribution to the kinetic energy and to the temperature variance. Besides, recent experiments by Schon (1974) in a thermal boundary layer with unstable stratification appear to corroborate roughly this proposed analogy.

The departure from the analogy appears to occur roughly at frequencies higher than the dissipation frequency N_1. This fact has been emphasized in the figures where the wavenumbers $(k_1)_d = 2\pi N_1/\bar{u}_1$ were used explicitly. It appears that at the highest frequencies the F_θ spectrum lies above the Q spectrum. This is a little surprising, if we consider that the molecular Prandtl number is less than unity. The spectra given for the highest frequencies are believed to be accurate since the experimental data obtained were compared with other measurements (see figure 5). As well, the above results are consistent with the fact that the peak of the production cospectrum $P_{\theta,2}$ was shifted towards the highest frequencies with respect to the velocity production cospectrum $P_{1,2}$, as shown on figure 11.

4. Relationship between the turbulent kinetic energy and the variance of temperature fluctuations

The spectral analogy which has been developed, emphasizes the importance of $\overline{q'^2}$ *vs.* $\overline{\theta'^2}$. On the other hand the moments of the turbulent quantities are often related to the gradients of the mean values by an explicit or implicit assumption of gradient diffusion. Therefore the ratio

$$B = \left(\frac{\overline{q'^2}}{\overline{\theta'^2}}\right)^{\frac{1}{2}} \left| \frac{\partial \bar{\theta}}{\partial y} \middle/ \frac{\partial \bar{u}_1}{\partial y} \right|$$

was calculated and plotted on figure 12. This demonstrates that $B \simeq 1{\cdot}5$, remaining nearly constant across most of the boundary layer, $0{\cdot}04 \lesssim y/\delta \lesssim 0{\cdot}8$. Very near the wall, the present measurements are incomplete but we may remark that at the wall, i.e. in the limit as $y \to 0$,

$$B = Pr \lim_{y \to 0} \frac{(\overline{q'^2})^{\frac{1}{2}}}{u_*} \Big/ \frac{(\overline{\theta'^2})^{\frac{1}{2}}}{\theta_*},$$

where $Pr = \mu c_p/k$ is the molecular Prandtl number.

The experiments of Elena (1975) also indicate that the limiting value of B is 1·5. Indeed, according to his data at $y^* \simeq 1{\cdot}5$, $(\overline{q'^2})^{\frac{1}{2}} u_*^{-1} \theta^*/(\overline{\theta'^2})^{\frac{1}{2}} = 2$ and $Pr \simeq 0{\cdot}73$. So B appears to be constant in the entire boundary layer except for the outer intermittent zone ($y/\delta \gtrsim 0{\cdot}8$), where results are rather uncertain.

Recalling the most common forms for the turbulent transfer terms,

$$-\overline{u_1' u_2'} = a\overline{q'^2} \quad \text{(Townsend 1956, p. 98)},$$

$$\overline{\theta' u_2'} = a_\theta[\overline{\theta'^2}(-\overline{u_1' u_2'})]^{\frac{1}{2}} \quad \text{(Bradshaw, Ferriss \& Atwell 1967)},$$

one obtains $B = Pr_t a_\theta/\sqrt{a}$, where Pr_t is the Prandtl number of the turbulence:

$$Pr_t = \frac{\overline{u_1' u_2'}}{\overline{\theta' u_2'}} \frac{\partial \bar{\theta}/\partial y}{\partial \bar{u}_1/\partial y}.$$

It appears, from the available experimental data, that the assumption that B is constant across the layer is much better than the usual assumptions that a, a_θ and Pr_t are constant.

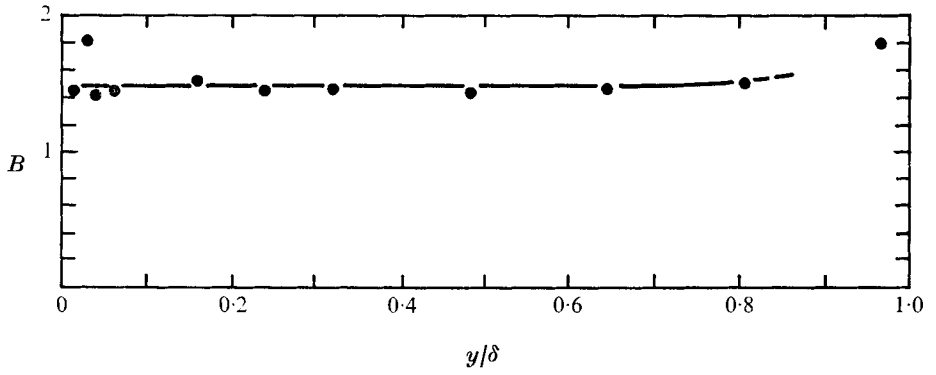

FIGURE 12. Variation of $B = (\overline{q'^2}/\overline{\theta'^2})^{\frac{1}{2}} |\partial\bar{\theta}/\partial y|/(\partial\bar{u}_1/\partial y)$ in the boundary layer.

5. Conclusions

An experimental investigation has been carried out in order to establish an analogy between the turbulent temperature and velocity fluctuations in a low Reynolds number boundary layer. For the comparison, spectral analysis was used, concentrating especially on the low frequency range that contains the major portion of the variance for the fluctuations considered. In this low frequency range, the previously used scalar mixing formulae do not provide satisfactory analogies. Thus an experimental study was needed.

The spectra of the temperature fluctuations and of the turbulent velocity components were measured across the boundary layer from $y_* = 16$ outwards to positions well into the intermittent zone. The cospectra between temperature and velocity fluctuations were also measured in some selected cases.

The principal results obtained are as follows.

(i) The temperature spectrum F_θ differs strongly from the spectrum F_1 of the longitudinal velocity component, except in the buffer layer, and is shifted towards the higher frequencies.

(ii) In the lowest frequency range the cospectra show that the temperature fluctuation θ' is strongly correlated with the streamwise velocity component, but at higher frequencies θ' becomes correlated with u_2', the velocity component normal to the wall.

(iii) Within the region of the logarithmic mean velocity profile, the spectral relation of Tchen (k_1^{-1}) has a moderate range of validity for $F_1(k_1)$. Because of the strong correlation of θ' with the streamwise velocity component, the spectrum F_θ exhibits similar behaviour, but in a much smaller frequency range.

(iv) The experiments have established rather conveniently the spectral analogy between the temperature spectrum F_θ and a velocity spectrum Q. The latter is defined as the sum of the three velocity-components spectra weighted by their relative variances. This finding is equivalent to the similarity between the autocorrelation $\overline{\theta'(t)\,\theta'(t+\tau)}$ and the autocorrelation of the velocity vector $\overline{\mathbf{v}'(t).\mathbf{v}'(t+\tau)}$. Measurements demonstrate that, throughout the boundary layer,

the spectra F_θ and Q are similar for the lower frequency range that includes about 80% of the variance.

(v) The analogy suggests the definition of a non-dimensional parameter

$$B = \left(\frac{\overline{q'^2}}{\overline{\theta'^2}}\right)^{\frac{1}{2}} \Big/ \left|\frac{\partial\bar{\theta}/\partial y}{\partial\bar{u}_1/\partial y}\right|,$$

which appears to be constant across the boundary layer, except perhaps in the strong intermittency zone. The experimental evidence obtained can be used to reinforce the prediction methods for heated turbulent boundary layers.

REFERENCES

ALEXOPOULOS, C. C. & KEFFER, J. F. 1968 *Toronto Univ. Rep.* UTME-TP 6810.

ANTONIA, R. A. 1974 *Proc. 5th Int. Heat Transfer Conf.*, p. 2.

BATCHELOR, G. K. 1952 *Proc. Roy. Soc.* A **213**, 349.

BRADSHAW, P., FERRISS, D. H. & ATWELL, N. P. 1967 *J. Fluid Mech.* **28**, 593.

BREMHORST, K. & BULLOCK, K. J. 1970 *Int. J. Heat Mass Transfer*, **13**, 1313.

CORRSIN, S. 1951 *J. Appl. Phys.* **22**, 461.

CORRSIN, S. & UBEROI, M. S. 1949 *N.A.C.A. Tech. Note*, no. 1865.

CORRSIN, S. & UBEROI, M. S. 1950 *N.A.C.A. Tech. Note*, no. 2124.

DUMAS, R. 1964 *Publ. Sci. Tech. Minist. Air*, no. 404.

DUMAS, R., FULACHIER, L. & ARZOUMANIAN, E. 1972 *C. R. Acad. Sci. Paris*, A **274**, 267.

ECKERT, E. R. G. & DRAKE, R. M. 1959 *Heat and Mass Transfer*. MacGraw-Hill.

ELENA, M. 1975 Thesis, Université d'Aix-Marseille II.

FAVRE, A. 1975 *Proc. 5th Can. Cong. Appl. Mech., Fredericton.*

FAVRE, A., DUMAS, R. & VEROLLET, E. 1968 *Proc. 12th Int. Congr. Appl. Mech.*, p. 192.

FAVRE, A. & GAVIGLIO, J. 1960 *Meeting AGARD Rep.* no. 278.

FREYMUTH, P. & UBEROI, M. S. 1971 *Phys. Fluids*, **14**, 2574.

FREYMUTH, P. & UBEROI, M. S. 1973 *Phys. Fluids*, **16**, 161.

FULACHIER, L. 1971 *C. R. Acad. Sci. Paris*, **272**, 1022.

FULACHIER, L. 1972 Thesis, Université de Provence, Marseille.

FULACHIER, L. & DUMAS, R. 1971 *Meeting AGARD Rep.* no. 93.

GAVIGLIO, J. 1962 *Publ. Sci. Tech. Minist. Air*, no. 385.

HOWARTH, L. 1953 *Modern Development in Fluid Dynamics, High Speed Flow*, vol. 2. Oxford: Clarendon Press.

JOHNSON, D. S. 1955 *Johns Hopkins Univ. Rep.* OSR TN 55–289.

KESTIN, J. & RICHARDSON, P. D. 1963 *Int. J. Heat Mass Transfer*, **6**, 147.

KLEBANOFF, P. S. 1954 *N.A.C.A. Tech. Note*, no. 1247.

KOVASZNAY, L. S. G. 1953 *N.A.C.A. Tech. Note*, no. 2939.

KOVASZNAY, L. S. G. & ALI, S. F. 1974 *Proc. 5th Int. Heat Transfer Conf.*, p. 2.

LUMLEY, J. L. & PANOFSKY, H. A. 1964 *The Structure of Atmospheric Turbulence*. Wiley.

OBOUKHOV, A. M. 1949 *Izv. Akad. Nauk SSSR, Geogr. Geophys. Ser.* **13**, 58.

PAO, Y. H. 1965 *Phys. Fluids*, **8**, 1063.

REYNOLDS, O. 1874 *Proc. Lit. Phil. Soc. Manchester*, **14**, 7.

RIBAUD, G. & BRUN, E. 1942 *Mem. Sci. Phys.* no. 46.

SCHON, J. P. 1974 Thesis, Université Cl. Bernard, Lyon.

TOWNSEND, A. A. 1956 *The Structure of Turbulent Shear Flow*. Cambridge University Press.

VEROLLET, E. 1969 *Publ. Sci. Tech. Minist. Air*, no. 449.

VEROLLET, E. 1972 Thesis, Université de Provence, Marseille.

VEROLLET, E. & FULACHIER, L. 1969 *C. R. Acad. Sci. Paris*, **268**, 1577.

VEROLLET, E. & FULACHIER, L. 1970 *C. R. Acad. Sci. Paris*, **270**, 1342.